

## MAGNETIC PROPERTIES OF SPUTTERED COBALT FILMS ON X-RAY LITHOGRAPHIC SUBSTRATES

P. SUKONRAT<sup>a</sup>, C. SIRISATHITKUL<sup>b\*</sup>, W. RATTANASAKULTHONG<sup>a</sup>,  
P. JANTARATANA<sup>a</sup>, C. SRIPHUNG<sup>c</sup>

<sup>a</sup> *Department of Physics, Faculty of Science, Kasetsart University, Bangkok 10900, Thailand*

<sup>b</sup> *Molecular Technology Research Unit, School of Science, Walailak University, Nakhon Si Thammarat, 80161, Thailand*

<sup>c</sup> *Synchrotron Light Research Institute (Public Organization) Nakhon Ratchasima, 30000, Thailand*

Arrays of 11.2-16.6  $\mu\text{m}$  holes were patterned on 50  $\mu\text{m}$  thick SU-8 photoresist layers by using synchrotron X-ray lithography. After the resist development, the chemically stable and mechanically hardened SU-8 templates with varying hole sizes were used as substrates for RF sputtering of 1.5  $\mu\text{m}$ -thick cobalt (Co). By comparing hysteresis loops from in-plane and out-of-plane magnetisation, the Co film on patterned substrate with average hole size of 16.6  $\mu\text{m}$  was more isotropic than in the case of 15.3 and 11.2  $\mu\text{m}$ . Both magnetic squareness and coercive field were at the minimum when the holes were smallest. After the removal of Co on SU-8 surfaces, the remaining Co deposits in the holes exhibited smaller squareness and anisotropy. On the other hand, the enhanced coercive field was increased with a reduction in diameter of patterned holes.

(Received November 28, 2014; Accepted December 29, 2014)

*Keywords:* X-ray lithography, Microhole array, SU-8 photoresist, Cobalt, Magnetic hysteresis

### 1. Introduction

Microscale patterned holes have been implemented in optoelectronic and magnetic devices. Metallic Al films with microholes arrays were studied for their applications as transparent electrodes [1]. For magneto-optical Dy-Fe-Co films, the depth of holes affected their domain structures and hence, magnetic properties [2]. On a nanoscale recording research, magnetic media were deposited in anodized aluminium oxide nanoholes [3,4]. Compared with continuous substrates, the coercive field of magnetic multilayers is enhanced by the depositions on patterned silicon [5,6]. Polymer templates are also effective for subsequent growth of photonic and magnetic materials. Zinc oxide nanorods highly oriented by polymethyl methacrylate holes [8] and magnetic Co-Cr-Pt films on urethane acrylate pillars [7] are among examples. With slightly different configurations, patterned organic/inorganic composites with a well defined size and distribution of the ceramic phase can also be realised by incorporating polymer templates with nanoparticles [9]. To produce such templates by means of lithography, a pattern was transferred on to a layer of sensitive polymer resist by via the masked irradiation. Compared to electron beam and photolithography techniques, X-ray lithography can fabricate a larger patterned area within a shorter time. High-aspect-ratio structures with vertical sidewalls can also be created by the deep penetration of X-rays into photoresist layers [10] and stray fields from the magnetic deposits from different levels do not interfere with one another [11].

---

\*Corresponding author: chitnarong.siri@gmail.com

Following the growing interests in magnetic inorganic/organic composites [12, 13], the fabrications of patterned organic templates provide opportunities of controlling the size and position of magnetic clusters. Several kinds of photosensitive polymers can be patterned [14]. In this work, SU-8 negative tone photoresist whose main components are Bisphenol A Novolak epoxy oligomer and triarylsulfonium hexafluoroantimonate salt is chosen as templates for subsequent magnetic Co deposition due to its high sensitivity to X-ray and good mechanical properties [15].

## 2. Experimental

### 2.1 X-ray lithographic mask

Each X-ray mask was produced from a graphite sheet polished to the thickness of  $250\ \mu\text{m}$  and coated by thin layers of titanium and silver (Fig.1a). A layer of  $15\ \mu\text{m}$  AZ4620 photoresist was then spin-coated on the graphite substrate (Fig.1b). The photoresist was soft-baked in an oven for 150 min and dried at room temperature for 24 h. A pattern of  $10\ \mu\text{m} \times 10\ \mu\text{m}$  square arrays with  $20\ \mu\text{m}$  spacing between the centres on an ultraviolet (UV) chrome mask was transferred to the photoresist by the UV irradiation of wavelength 365 nm for 90 s (Fig. 1c). After immersion in an AZ developer for 3 min, the pattern emerged on the graphite mask (Fig. 1d) and it was covered by electroplated silver using a current density of  $1\ \text{mA}/\text{cm}^2$  for 30 min (Fig.1e). Since their corners are curved, the silver dots are almost spherical with a diameter about  $10\ \mu\text{m}$ .

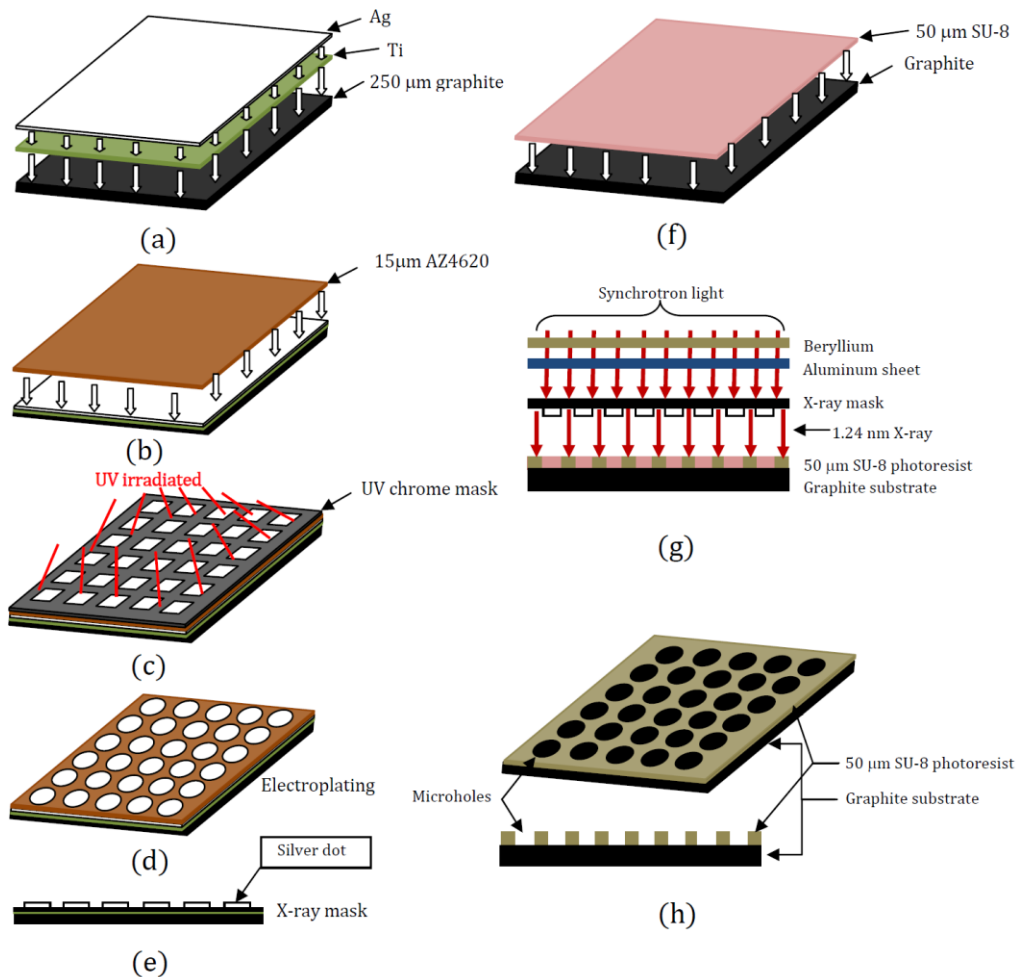


Fig. 1. Diagram of preparation procedure for the patterned microhole template.

## 2.2 SU-8 microhole templates

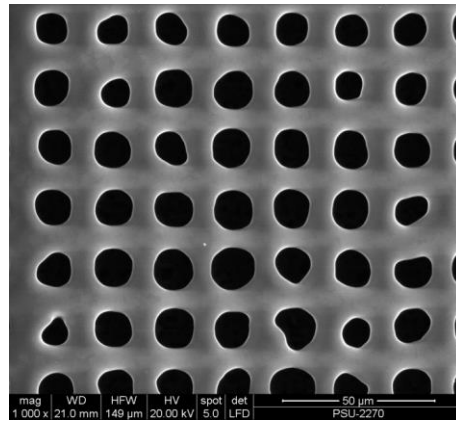
The X-ray exposure was performed at the beam line BL6a of the Synchrotron Light Research Institute, Thailand. Pieces of graphite spin-coated with a layer of 50  $\mu\text{m}$  thick SU-8 were used as substrates for the masked irradiation (Fig. 1f). These substrates were soft-baked at 95  $^{\circ}\text{C}$  for 40 min to remove the solvent and improve the adhesion between layers and then dried at room temperature for 24 h before the exposure. In a pattern transfer from the graphite mask to a layer of SU-8, X-ray of wavelength 1.24 nm was irradiated onto the substrate placed under the mask for 10 min (Fig. 1g). The exposed resist in an area about 5 mm  $\times$  5 mm was then left at room temperature for 24 h before developing. The arrays of microholes on SU-8 resist layer (Fig. 1h) were finally inspected by a scanning electron microscopy (SEM). The distribution in size was expressed in terms of average diameter and its standard deviation from 36 holes in each sample. Moreover, the image processing can be implemented to determine the size of these patterned holes [16].

## 2.3 Co films on microhole substrates

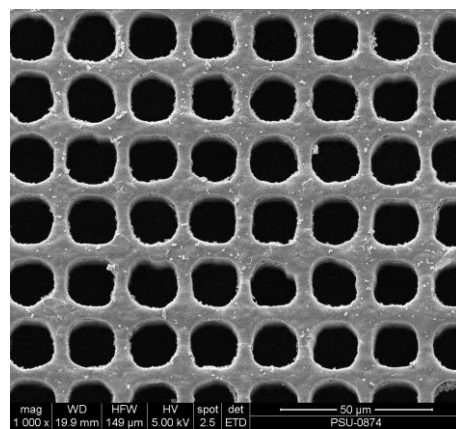
The patterned templates were used as substrates in the 300 W RF sputtering of 1.5  $\mu\text{m}$  thick Co. The sputtering chamber was filled with argon gas of 33 sccm. The coated samples were then polished to remove Co from the surface of SU-8 template. The surface morphology of samples was inspected by SEM. Their magnetic properties were measured by vibrating sample magnetometry (VSM) in both in-plane and out-of-plane magnetisation. The magnetic field is applied parallel to the surface of Co deposits in the in-plane configuration whereas the magnetic field is perpendicular to the Co surface in the out-of-plane magnetisation. The coercive field is determined from an x-intercept of the hysteresis loop and the squareness is a ratio of the remanent magnetisation obtained from a y-intercept of the loop to the saturation magnetisation.

## 3. Results and discussion

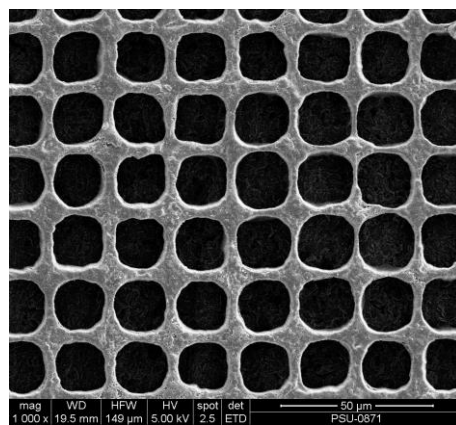
Fig. 2 shows patterned SU-8 layers on graphite substrates. In SEM micrographs, the dark cross-sectional areas represent the holes originating from the SU-8 resist covered by the lithographic mask during the X-ray exposure. For the SU-8 exposed to X-ray, triarylsulfonium hexafluoroantimonate salt decomposed and reacted with epoxy oligomer [15] and the induced cross-linking reduced its solubility to the developer. It follows that only hardened SU-8 remained on the graphite substrate while the unexposed SU-8 was washed away. Imperfect resist developments and rinsing as well as heat treatments evidently led to three samples of different hole sizes in Fig. 2. The diameter of the hole cross section averaged from 36 holes in these samples are  $11.2 \pm 1.2$ ,  $15.3 \pm 0.7$  and  $16.6 \pm 1.0$   $\mu\text{m}$ . After the Co deposition, SEM micrographs in Fig. 3 indicate the increased roughness compared to the smooth templates before deposition in Fig. 2. The contrast between the surface and the bottom of the holes is reduced because of Co deposits in both SU-8 surfaces and holes.



(a)

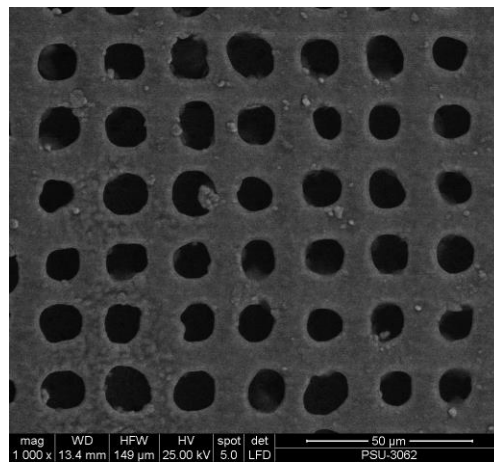


(b)

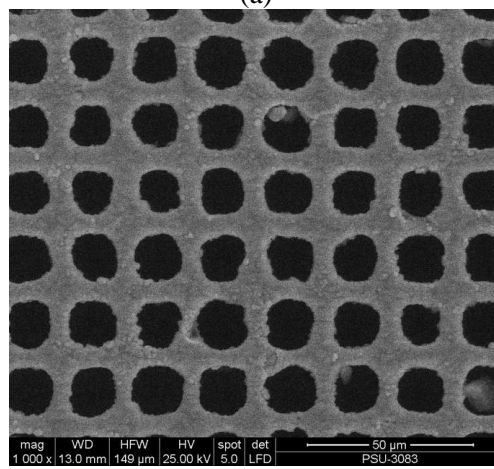


(c)

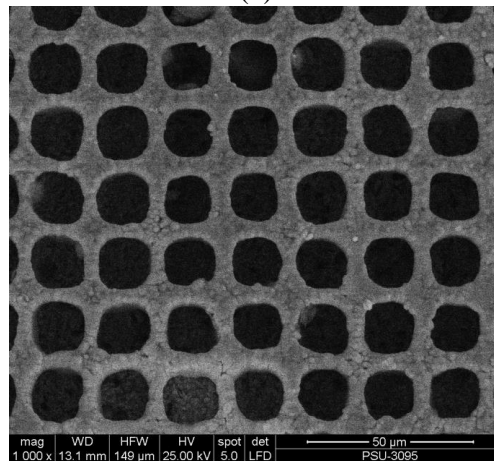
*Fig. 2. SEM micrographs of patterned templates with average hole size of (a) 11.2, (b) 15.3 and (c) 16.6  $\mu\text{m}$ .*



(a)



(b)



(c)

*Fig. 3. SEM micrographs of Co films on patterned substrates with average hole size of (a) 11.2, (b) 15.3 and (c) 16.6  $\mu\text{m}$*

In Figs. 4-6, hysteresis loops of Co films on hole-patterned substrates are normalised to the saturation in-plane magnetisations. When a magnetic field is increasingly applied in parallel to the Co surface, the in-plane magnetisation is initially increased with a high rate but its sensitivity to the change in magnetic field beyond 2000 Oe is reduced as the saturation is approached. By applications of magnetic field in the perpendicular direction to the Co surface, the out-of-plane

magnetisation rises with a slower rate to a lower value in 5500 Oe field. A higher magnetic field is apparently needed to saturate the magnetisation in this direction. Interestingly, the anisotropic behavior is less pronounced in the case of the larger holes in Figs. 5-6. It implies that the anisotropy is increasingly developed when the magnetic film is deposited in the holes of smaller cross-sectional areas. Without Co on the SU-8 surface after polishing, the remaining Co deposits in microholes exhibit reduced magnetisations. The preference for in-plane magnetisation is still observed but the difference between in-plane and out-of-plane magnetisation is decreased. It is confirmed that the anisotropic contribution is largely belong to Co deposits on the SU-8 surface.

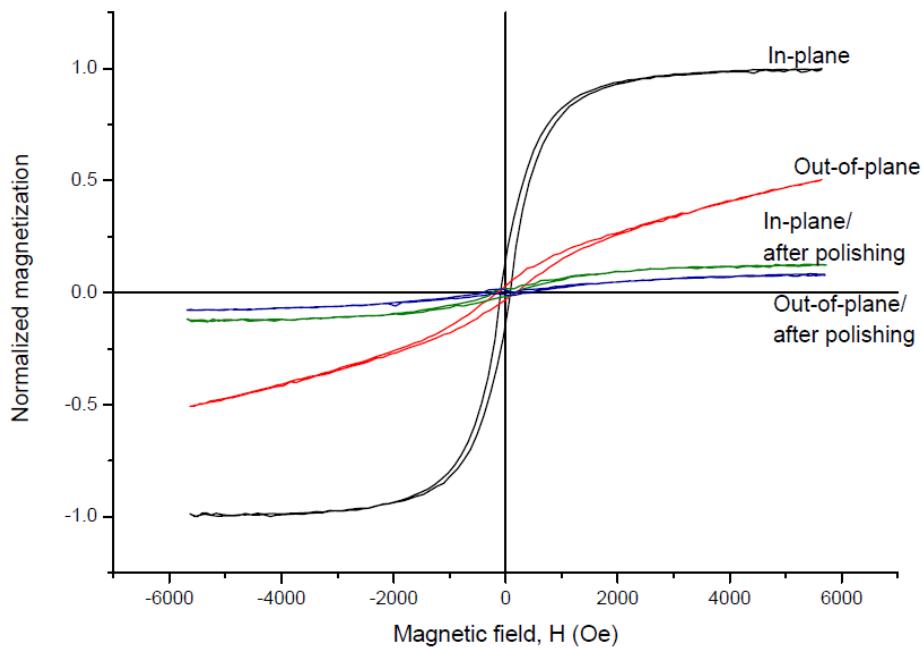


Fig. 4. Hysteresis loops of Co film on patterned substrate with average hole size of  $11.2 \mu\text{m}$

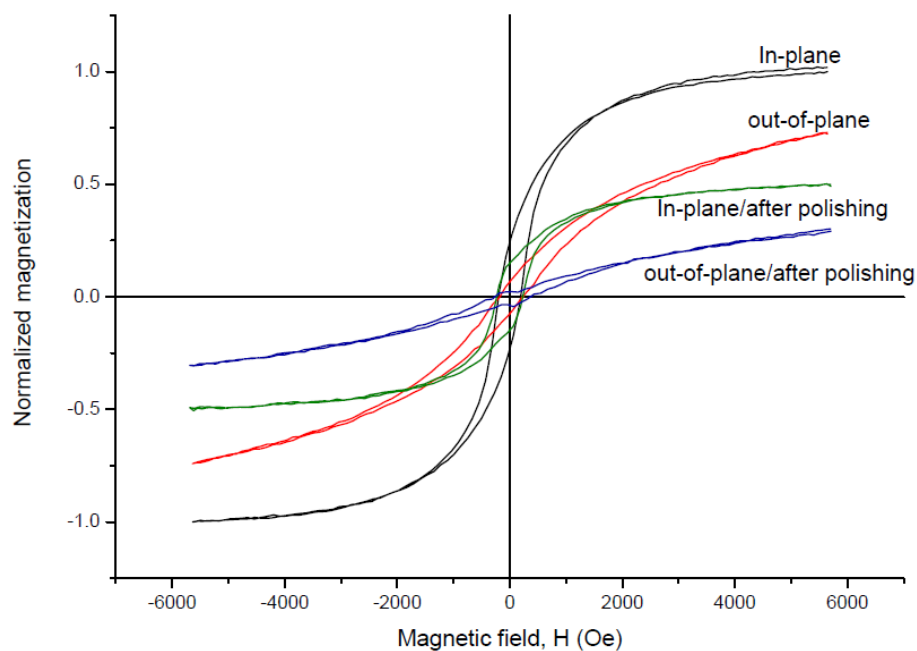


Fig. 5. Hysteresis loops of Co film on patterned substrate with average hole size of  $15.3 \mu\text{m}$

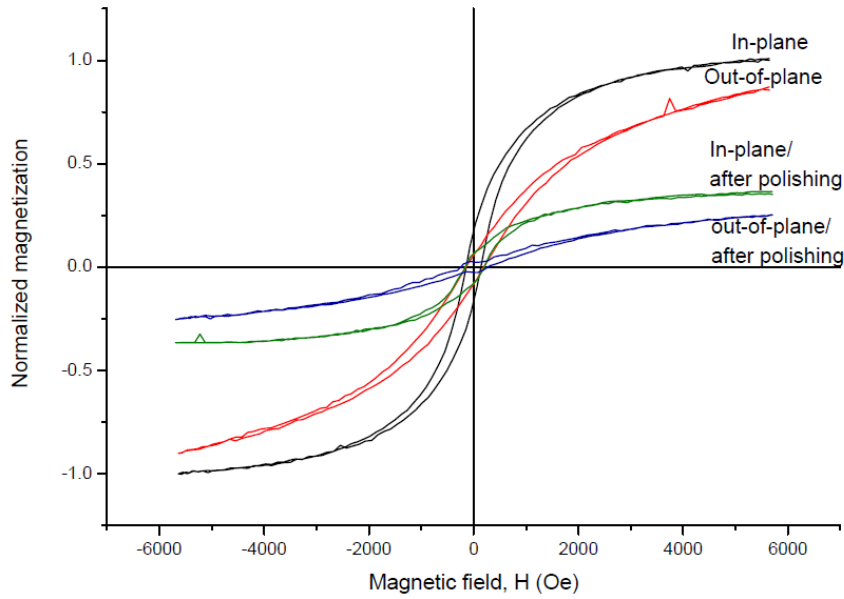


Fig. 6. Hysteresis loops of Co film on patterned substrate with average hole size of  $16.6 \mu\text{m}$

The coercive field (Fig. 7) and magnetic squareness (Fig. 8) determined from in-plane and out-of-plane hysteresis loops are plotted as a function of the hole size. Before polishing, the direction of applied magnetic field has the smallest effect on coercive field and squareness when the hole size is at the maximum reflecting the relatively isotropic hysteresis loops in Fig. 6. In both in-plane and out-of-plane cases, the coercive field and squareness are minimal in the case of  $11.2 \mu\text{m}$  and reach the maximum in the case of  $15.3 \mu\text{m}$ . By considering two contributions from Co in the holes and Co on SU-8 surface, the sizes of magnetic deposits are comparable in the case of  $15.3 \mu\text{m}$  hole. Larger Co deposits either in  $16.6 \mu\text{m}$  holes or on SU-8 surface in the case of  $11.2 \mu\text{m}$  lead to the overall reduction in coercive field.

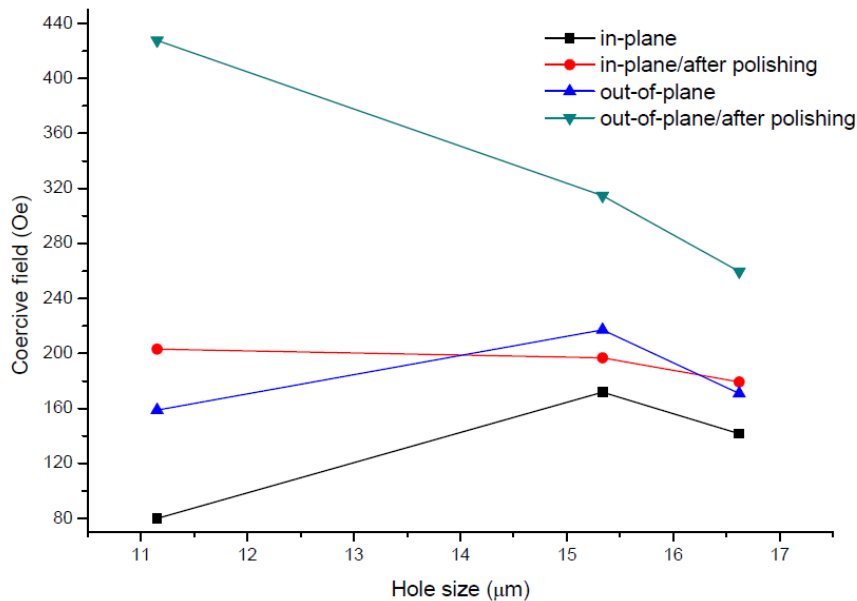


Fig. 7. Coercive field of Co films on patterned substrates with varying hole sizes before and after polishing

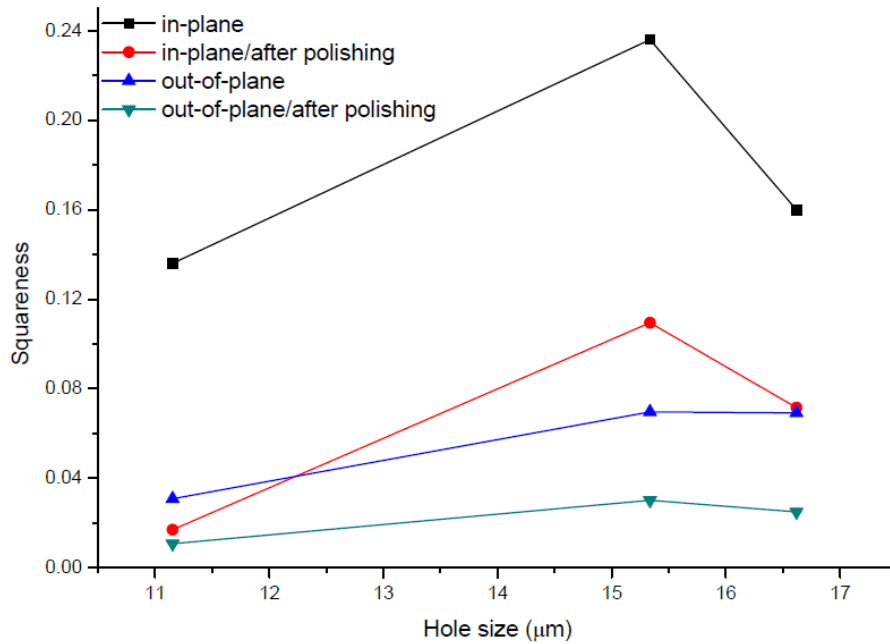


Fig. 8. Magnetic squareness of Co films on patterned substrates with varying hole sizes before and after polishing

Without Co on SU-8 surface, the squareness is decreased and the variation in squareness with the hole size resembles that before polishing with a smaller difference between the in-plane and out-of-plane configurations. By contrast, the coercive field after polishing is increased with a much higher out-of-plane value than the in-plane counterpart. Unlike before polishing, the coercive field are clearly decreased with the increase in the hole size. The trend can be understood by emphasising that the coercive field after polishing is solely contributed by the Co deposits in the holes. In the microscale down to a certain nanoscale range, the smaller magnetic structures are harder to demagnetise and the coercive field is increased with the reduction in size [17]. The result in Fig. 7 also agrees with the previous observation by Ye *et al.* that the coercive field of magnetic deposits in patterned holes is larger than that of the surface area [2].

#### 4. Conclusions

It was demonstrated that properties of magnetic microstructure can be controlled by the size distribution of X-ray lithographic patterns. Microholes with a depth of 50 μm were patterned on SU-8 photoresist layer by X-ray lithography using the synchrotron radiation. After RF sputtering of 1.5 μm-thick Co, magnetisations were highly anisotropic in respect to the direction of applied magnetic field in the case of the minimum hole size. With increasing hole size, the coercive field and magnetic squareness were increased. After Co deposits were removed from SU-8 surfaces and left only in patterned holes, magnetisations were reduced and became more isotropic. In contrast to the squareness, the enhanced coercive field was decreased by an increase in the hole size.

## Acknowledgements

This work is funded by the Thailand's Synchrotron Light Research Institute (Grant 2552/PS01). The micrographs were taken at Scientific Equipment Center, Prince of Songkla University.

## References

- [1] X.-L. Zou, Z.-J Sun, *Optoelectron. Adv. Mater. Rapid Commun.* **4**, 647, (2010).
- [2] L. X. Ye, J. M. Lee, J. C. Wu, T.-H. Wu, *IEEE Trans. Magn.* **41**, 956, (2005).
- [3] A. I. Gapin, X. R. Ye, L. H. Chen, D. Hong, S. Jin, *IEEE Trans. Magn.* **43**, 2151 (2007).
- [4] H. Oshima, H. Kikuchi, H. Nakao, K. Itoh, T. Kamimura, T. Morikawa, K. Matsumoto, T. Umada, H. Tamura, K. Nishio, H. Masuda, *Appl. Phys. Lett.* **91**, 022508 (2007).
- [5] K. Noh, C. Choi, H. Kim, Y. Oh, J.-Y. Kim, D. Hong, L.-H. Chen, S. Jin, *IEEE Trans. Magn.* **47**, 3478 (2011).
- [6] V. Baltz, S. Landis, B. Rodmacq, B. Dieny, *J. Magn. Magn. Mater.* **290-291**, 1286 (2005).
- [7] J. B. Cui, *Sci. China Ser. E-Tech. Sci.* **52**, 313 (2009).
- [8] J. Han, J. M. Yang, S. C. Shin, Y.-J. Kim, S. Kang, *IEEE Trans. Magn.* **45**, 2288 (2009).
- [9] S. S. Andrade, D. Rabelo, V. K. Garg, A. C. Oliveira, P. C. Morais, *J. Magn. Magn. Mater.* **289**, 25 (2005).
- [10] A. del Campo, E. Arzt, *Chem. Rev.* **108**, 911 (2008).
- [11] C. Choi, D. Hong, Y. Oh, K. Noh, J. Y. Kim, L. Chen, S. H. Liou, S. Jin, *Elec. Mater. Lett.* **6**, 113 (2010).
- [12] A. M. Atta, G. A. El-Mahdy, H. A. Al-Lohedan, S. A. Al Hussain, *Dig. J. Nanomat. Biostruct.* **9**, 627 (2014).
- [13] N. Thangaraj, K. Tamilarasan, D. Sasikumar, *Dig. J. Nanomat. Biostruct.* **9**, 27 (2014).
- [14] M. Kitsara, D. Goustouridis, E. Valamontes, P. Oikonomou, K. Beltsios, I. Raptis, *J. Optoelectron. Adv. Mater.* **12**, 1147 (2010).
- [15] A. del Campo, C. Greiner, *J. Micromech. Microeng.* **17**, R81 (2007).
- [16] U. Phromsuwan, Y. Sirisathitkul, C. Sirisathitkul, P. Muneesawang, B. Uyyanonvara, *MAPAN-J. Metrol. Soc. India* **28**, 327 (2013).
- [17] G. Gubbiotti, L. Albini, G. Carlotti, M. De Crescenzi, E. Di Fabrizio, A. Gerardino, O. Donzelli, F. Nizzoli, H. Koo, R. D. Gomez, *J. Appl. Phys.* **87**, 5633, (2000).